Journal of Oceanography, Vol. 61, pp. 987 to 993, 2005

Short Contribution

Altimeter Measurements of Wind and Wave Modulation by the Kuroshio in the Yellow and East China Seas

PAUL A. HWANG*

Oceanography Division, Naval Research Laboratory, Stennis Space Center, MS 39529-5004, U.S.A.

(Received 28 December 2004; in revised form 17 February 2005; accepted 14 March 2005)

The Kuroshio is the major ocean current conveying heat and water mass in the Pacific Ocean. The impact of the Kuroshio on regional wind and wave distributions has been studied with spaceborne-altimeter measurements in the Yellow and East China Seas. In this region the Kuroshio trajectory is relatively stationary and the monsoon patterns dominate, making it an ideal natural laboratory for large scale air-sea-current interaction research. Major findings from this study include: (a) The Kuroshio exerts significant influence on the wind and wave distributions over a swath about 800-km wide along its path. (b) Seasonal average wind speeds reach a maximum near the Kuroshio axis. The magnitude of enhancement ranges between 20 and 50 percent. (c) The distribution of the surface wave heights displays similar spatial patterns to the wind-speed distribution. The Kuroshio effects on wave heights are further complicated by the hydrodynamic modulation of wave-current interaction and the influence of thermal stratification on wind-wave generation. (d) Kuroshio effects are most prominent in the first and last quarters of the year, and least prominent in the third quarter.

Keywords:
· Air-sea-current interaction,
· Kuroshio,
· modulation,
· wave-current interaction,
· stability.

1. Introduction

Spaceborne altimeters provide measurements of wind speed, U_{10}, and significant wave height, H_s, at intervals of about 7 km along the satellite ground tracks. Comparison studies of the altimeter-measured wind speeds and wave heights with surface buoy data have shown good agreement (e.g., Freilich and Challenor, 1994; Gower, 1996; Hwang *et al.*, 1998a; Queffeulou, 2003, 2004). The synoptic data can be used to produce seasonal and annual wind and wave climatologies to one-degree resolution (e.g., Hwang and Teague, 1998) and to investigate the spatial patterns of wind and wave distributions in regional scales (e.g., Hwang *et al.*, 1999). Synoptic pictures of the seasonal climatology of winds and waves constructed from the TOPEX data (e.g., figure 2 of Hwang *et al.*, 1998b) show abundant details of spatial structures. One of the most interesting features is the local intensification of the wind and wave distributions along the Kuroshio axis as described by Hwang *et al.* (1998b). The unambiguous enhancement is much more difficult to detect in other regions based on examinations of the wind and wave distributions along ground tracks crossing the Kuroshio or the Gulf Stream in various locations. It is assumed that for such features to become manifest in measurements, a stable path of the major ocean current and reasonably persistent weather patterns in the area of investigation are required. The Kuroshio in the East China Sea is confined by the bathymetry (Qiu and Imasato, 1990; Sun and Su, 1994; Lie *et al.*, 1998). The relatively stable course of the Kuroshio, the regular monsoon weather patterns and the almost-closed boundaries of the region make it a natural laboratory for investigating regional scale air-sea-current interactions. This note presents analyses of the TOPEX data along a ground track following approximately the central axis of the Yellow and East China Seas (Section 2). The distributions of the seasonal averages of wind speeds and wave heights along the ground track are presented. Local enhancement of the average wind speeds attributing to the influence of the Kuroshio is quantified. A similar pattern of wave-height enhancement is found along the ground track. In additional to the direct correlation of wind-speed enhancement with the wave-height enhancement, the modification of the wave-height distribution is further complicated by the mechanism of wave-

* E-mail address: paul.hwang@nrlssc.navy.mil

REPORT DOCUMENTATION PAGE

Form Approved
OMB No. 0704-0188

1. REPORT DATE *(DD-MM-YYYY)*	2. REPORT TYPE	3. DATES COVERED *(From - To)*
6-06-2006	Journal Article (refereed)	

4. TITLE AND SUBTITLE
Altimeter Measurements of Wind and Wave Modulation by the Kuroshi in the Yellow and East China Seas

5a. CONTRACT NUMBER

5b. GRANT NUMBER

5c. PROGRAM ELEMENT NUMBER
PE0601153N

6. AUTHOR(S)
Paul A. Hwang

5d. PROJECT NUMBER

5e. TASK NUMBER

5f. WORK UNIT NUMBER
73-8190-04

7. PERFORMING ORGANIZATION NAME(S) AND ADDRESS(ES)
Naval Research Laboratory
Oceanography Division
Stennis Space Center, MS 39529-5004

8. PERFORMING ORGANIZATION REPORT NUMBER
NRL/JA/7330-04-20

9. SPONSORING/MONITORING AGENCY NAME(S) AND ADDRESS(ES)
Office of Naval Research
800 N. Quincy St.
Arlington, VA 22217-5660

10. SPONSOR/MONITOR'S ACRONYM(S)
ONR

11. SPONSOR/MONITOR'S REPORT NUMBER(S)

12. DISTRIBUTION/AVAILABILITY STATEMENT
Approved for public release, distribution is unlimited.

13. SUPPLEMENTARY NOTES

14. ABSTRACT
The Kuroshio is the major ocean current conveying heat and water mass in the Pacific Ocean. The impact of the Kuroshio on regional wind and wave distributions has been studied with spaceborne-altimeter measurements in the Yellow and East China Seas. In this region the Kuroshio trajectory is relatively stationary and the monsoon patterns dominate, making it an ideal natural laboratory for large scale air-sea-current interaction research. Major findings from this study include: (a) the Kuroshio exerts significant influence on the wind and wave distributions over a swath about 800-kim wide along its path. (b) Seasonal average wind speeds reach a maximum near the Kuroshio axis. The magnitude of enhancement ranges between 20 and 50 percent. (c) The distribution of the surface wave heights displays similar spatial patterns to the wind-speed distribution. The Kuroshio effects on wave heights are further complicated by the hydrodynamic modulation of wave-current interaction and the influence of thermal stratification on wind-wave generation. (d) Kuroshio effects are most prominent in the first and last quarters of the year, and least prominent in the third quarter.

15. SUBJECT TERMS
spaceborne altimeters; Kuroshio; wind and wave modulation; Yellow Sea; East China Sea

16. SECURITY CLASSIFICATION OF:			17. LIMITATION OF ABSTRACT	18. NUMBER OF PAGES	19a. NAME OF RESPONSIBLE PERSON
a. REPORT	b. ABSTRACT	c. THIS PAGE			Paul A. Hwang
Unclassified	Unclassified	Unclassified	UL	7	19b. TELEPHONE NUMBER *(Include area code)* (301) 412-4914

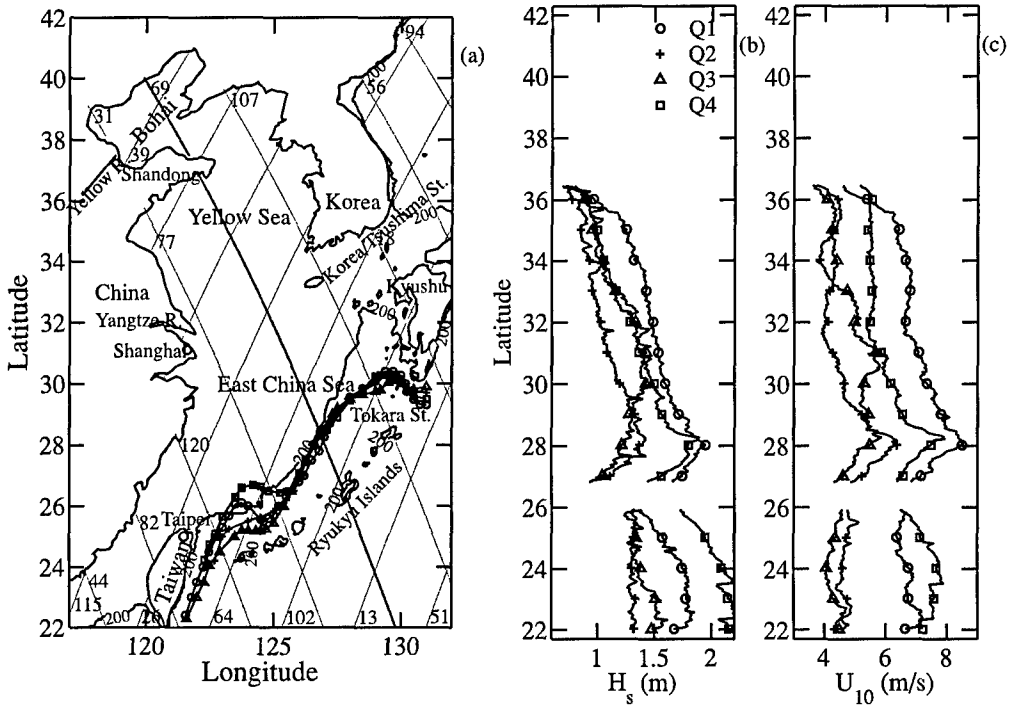

Fig. 1. Modulation of winds and waves by the Kuroshio. (a) TOPEX ground tracks in the Yellow and East China Seas, with ground track 69 highlighted. The seasonal variation of the Kuroshio axes are superimposed on the map (+: spring, △: summer, □: fall, ○: winter). The 200-m depth contour is also shown. Seasonal averages of (b) wave heights and (c) wind speeds along ground track 69. The results are based on four years average (1993–1996) of TOPEX outputs. The Kuroshio axes intersect ground track 69 at approximately 28°N. Local enhancements of wind speeds and wave heights are attributed to the Kuroshio influence.

current interaction and the effect of stability conditions on the generation of wind waves. The altimeter measurements are compared with numerical computations of wave modulation by a shear current using the action density conservation equation of surface waves. The growth function of wind-generated waves is used to estimate the effects of wind-speed distribution on the wave-height distribution. The contributions to the wave-height enhancement due to wave-current interaction and wind-speed distribution are found to be comparable: each contributes about one third to the observed level of the wave-variance enhancement attributable to the Kuroshio. The results suggest that the effect of unstable stratification on wind-wave generation accounts for the remaining one-third contribution to the observed wave-variance enhancement (Section 3). Finally, conclusions from this study are summarized in Section 4.

2. Modification of Winds and Waves by the Kuroshio

2.1 Data analysis

To evaluate the quantitative effects of the Kuroshio modulation of regional wind and wave properties, the original data from individual satellite ground tracks provide the highest spatial resolution. Examples of the cycle-by-cycle spatial distributions of H_s and U_{10} along ground track 69, which passes through the central portion of the region, can be found in figure 4 of Hwang *et al.* (1999). In the present analysis, the altimeter data (H_s and U_{10}) are first interpolated linearly onto uniform spacing of 0.05-degree latitude along the ground track. The distance between neighboring points of the interpolated dataset is between 6.0 and 6.3 km, slightly smaller than the nominal distance (7 km) of the original geophysical data record.

The seasonal mean trajectories of the Kuroshio in the ECS based on a geomagnetic electrokinetograph (GEK) survey (Sun and Su, 1994) are plotted in Fig. 1(a). The seasonal (quarter-year average) distributions of H_s and U_{10} along ground track 69 are shown in Figs. 1(b) and (c). The Kuroshio crosses ground track 69 at approximately 28°N (Fig. 1(a)). The wind and wave distributions show distinctive enhancement at the Kuroshio location (Figs. 1(b) and (c)). The results also reflect the climatology of the region. The primary wind direction in the winter months is northwesterly in the north (Bohai), north-

Table 1. Rate-of-increase of wind speeds (m/s per degree latitude) and wave heights (m per degree latitude) along ground track 69.

		27°N to axis	Axis to 29°N	29°N to 32°N	32°N to 34°N
Wave height	Q1	−0.22	0.25	0.10	0.07
	Q2	−0.20	0.25	0.11	0.11
	Q3	—	—	—	—
	Q4	−0.25	0.11	0.08	0.03
Wind speed	Q1	−1.4	0.7	0.4	~0
	Q2	−1.0	1.2	0.4	~0
	Q3	−1.2	—	—	—
	Q4	−1.4	1.5	0.3	~0

erly in the Yellow Sea (YS) and northeasterly in the ECS. In the summer, the wind direction is southerly to southeasterly in the whole region. The winds fluctuate during the transitional seasons (Wang and Aubrey, 1987).

It is clarified here that the U_{10} output from the altimeter is deduced from the ocean surface roughness, which is modified primarily by the wind speed, the atmospheric stability condition, and the ocean-surface current distribution. Weissman and Graber (1999) reported a comparison study showing that the wind friction velocity derived from the scattering cross section of a satellite scatterometer is in very good agreement with that obtained from buoy measurement using a bulk formula. In the vicinity of major ocean currents, such as the Kuroshio and the Gulf Stream, three is a significant contribution from atmospheric instability caused by the air-sea temperature difference, and the surface current speeds may be a significant fraction of the wind speeds. Conventionally, U_{10} represents the equivalent wind speed (on an inertial coordinate system) at 10-m elevation under neutral stability condition and may differ from the wind speed measured by an instrument mounted at 10-m elevation. In the presence of a strong current, such as the Kuroshio with a surface current speed of 1 to 2 m/s, the satellite-measured U_{10}, which is more useful for air-sea interaction studies than the anemometer wind speed, can be expected to be enhanced or retarded (depending on the direction between wind and current) by a magnitude similar to the surface current speed. Other known factors affecting the altimeter backscattering coefficient include the sea surface temperature, wave (surface roughness) modulation near current boundaries, and foam and whitecaps produced by breaking waves.

The Kuroshio modification on the wind-speed distribution is somewhat simpler than the modification on the wave-height distribution, and will be discussed first (Fig. 1(c)). The effect is especially strong in Q1 (January, February and March) and Q4 (October, November and December). For these two quarters, the wind speeds in the region north of 32°N are relatively constant, except in the region close to the coast. South of 32°N in the East China Sea, the average wind speeds increase steadily at a rate of 0.3 to 0.4 m/s per degree latitude from 32 to 29°N. Within approximately 100 km of the Kuroshio axis, the growth rate increases significantly, ranging from 0.7 to 1.2 m/s per degree latitude. After passing the Kuroshio axis, wind speed decreases at an even higher rate of −1 to −1.4 m/s per degree latitude (Table 1). The sharp rate-of-decrease in the last region is partially caused by the sheltering effect due to the presence of the Ryukyu Islands, which cross the ground track 69 at about 26.4°N. Q2 (April, May and June) is the transitional season in the region and the magnitudes of wind speeds and wave heights are much smaller than their counterparts in Q1 and Q4. The magnitude of modulation, however, is comparable to that of Q1 and Q4 (Table 1). In Q3 (July, August and September) when the southerly monsoon prevails in the region, a similar but smaller local enhancement in the wind-speed distribution at the Kuroshio location is also apparent, but the overall distribution is more irregular compared to that of the other three seasons. In particular, there are additional local peaks of the wind-speed distribution at about 30.5, 32.2 and 35.8°N, which will be further discussed in Subsection 2.2.

The distributions of the average wave height display many similar features of the distributions of the average wind speed, except that in the region of constant wind speeds north of 32°N and away from coastal influences, waves continue to increase due to fetch growth (assuming that the wind fetch increases southward in the three seasons Q1, Q2, and Q4). The rate-of-increase of wave heights in the vicinity of the Kuroshio is again two to three times larger than that in the region further away from the Kuroshio axis. The rate of wave-height increase is more than can be accounted for by the wind-speed enhancement (to be further quantified in Subsection 3.2). Table 1 lists the growth rate of winds and waves in the region between 27 to 34°N, divided into four general sub-

regions as described in the discussion of the wind-speed distributions.

2.2 Dynamic significance

One of the obvious mechanisms producing the observed local enhancement of wind speeds is the unstable atmospheric boundary layer above the Kuroshio. The unstable stratification generates vertical convection, which in turn enhances the horizontal air flow due to the continuity of the fluid motion. Based on the results shown in Fig. 1(c), the region of immediate influence of the Kuroshio on the wind-speed distribution is about 100 km on either side of the Kuroshio axis, and the extended influence reaches about 400 km from the axis. The Kuroshio effects on the region's atmospheric and oceanographic climatologies are obviously quite far-reaching and encompass a swath about 800-km wide along its path. The significant implications of the positive covariations of the sea surface temperature and surface wind speed on air-sea interaction processes have been discussed by Xie *et al.* (2002) and Nonaka and Xie (2003).

The observed wind-speed distributions in the summer months are of special interest as they reveal other frontal systems that have impacts comparable to the weakened Kuroshio effect in these months. As discussed earlier, there are additional local peaks in the wind-speed distribution at about 30.5, 32.2 and 35.8°N. Those locations seem to match the edges of the Yangtze Bank Ring Front (30.5, 32.2°N) and the Shandong Peninsula Front (35.8°N) described in figure 2 of Hickox *et al.* (2000) and figure 8 of Belkin and Cornillon (2003) (the latitudes in figure 8 of Belkin and Cornillon (2003) are off by 5°). There have been persistent questions about the source of the Yellow Sea Warm Current and whether it is a permanent feature (e.g., Nitani, 1972; Beardsley *et al.*, 1985; Lie *et al.*, 2001; Teague *et al.*, 2003). Results from remote sensing measurements, such as the frontal structure inferred from the SST data (Hickox *et al.*, 2000; Belkin and Cornillon, 2003) or the wind-speed modification by a heat source as presented above, may provide additional information for resolving such elusive questions. The results of the altimeter wind-speed modulation suggest that both the Yangtze Bank Ring Front and the Shandong Peninsula Front are more prominent in the spring and summer seasons and their signature is much weaker in the winter, possibly masked by the influence due to the Kuroshio. The close correlation between the sea surface temperature and the surface wind velocity in the Kuroshio regions has been reported by Xie *et al.* (2002) and Nonaka and Xie (2003). Using multiple satellite products, Xie *et al.* (2002) illustrated the profound influence of the bathymetric control on the SST distribution in the Yellow and East China Seas and the subsequent influence on the distributions of winds and clouds. Their analyses also illustrate the strong influence of the Kuroshio on the weather over the whole region of the Yellow and East China Seas.

3. Wave-Current Interaction

3.1 Numerical computation

In the neighborhood of the Kuroshio axis, additional enhancement of winds and waves is apparent. The wave-height enhancement upstream and the subsequent decrease downstream of the Kuroshio axis is a characteristic feature of the surface-wave modulation by current shear (e.g., Longuet-Higgins and Stewart, 1960; Keller and Wright, 1975; Hughes, 1978; Thompson and Gasparovic, 1986; Hwang and Shemdin, 1990; Hwang, 1999). The wave action density conservation equation can be used to quantify the current modulation of surface waves,

$$\frac{dN}{dt} = \frac{\partial N}{\partial t} + \frac{\partial N}{\partial \vec{x}}\frac{\partial \vec{x}}{\partial t} + \frac{\partial N}{\partial \vec{k}}\frac{\partial \vec{k}}{\partial t} = \sum Q_i, \tag{1}$$

where N is the wave action, t is time, $\vec{x} = (x, y)$ is the space vector, $\vec{k} = (k_1, k_2)$ is the wavenumber vector, and Q_i are source terms. The partial differential equation (1) can be transformed into a system of ordinary differential equations,

$$\frac{dN}{dt} = \sum Q_i, \tag{2}$$

$$\frac{d\vec{x}}{dt} = \vec{c}_g + \vec{U}, \tag{3}$$

$$\frac{d\vec{k}}{dt} = -k_1 \nabla U - k_2 \nabla V, \tag{4}$$

where $\vec{c}_g$ is the group velocity, and $\vec{U} = (U, V)$ is the current vector. Equations (2) to (4) can be solved by the method of characteristics (e.g., Hughes, 1978; Hwang and Shemdin, 1990). Because the wavelengths investigated here are relatively long, the magnitudes of the source functions of wind input and breaking dissipation—based on Plant's (1980) or Hughes' (1978) formulations, for example—are very small. Numerical experiments with or without source functions did not produce significant differences in the computational results. In the following discussions, all computations are based on zero external source terms. The only mechanism contributing to the modulation is the spatial variation of the surface velocity in the Kuroshio. For the modulation computation, the surface velocity is assumed to follow a 1D Gaussian profile,

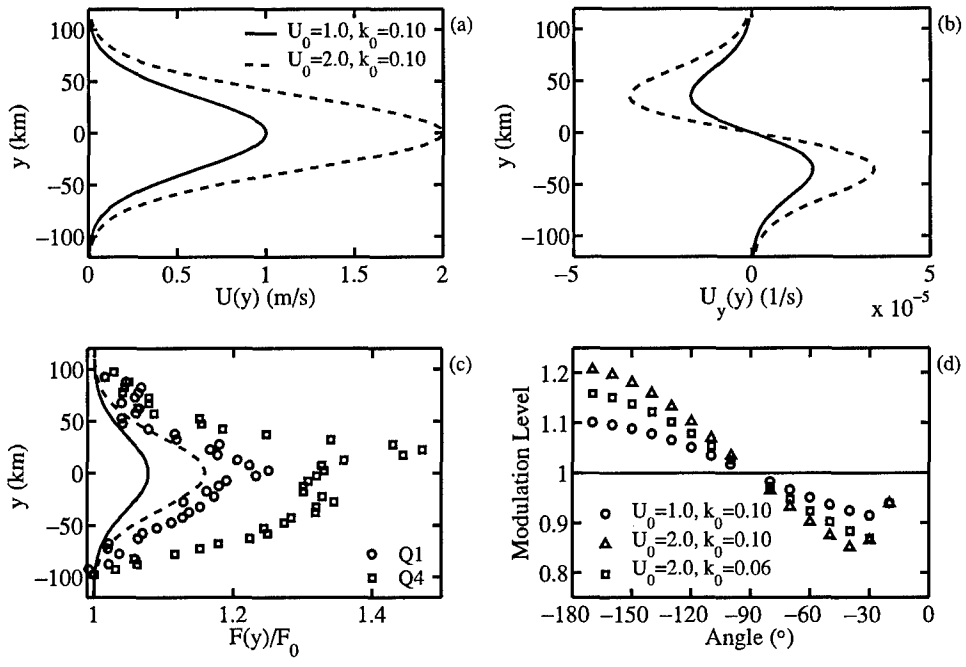

Fig. 2. Examples of the modulation computations. (a) Current profile, (b) current shear, (c) distribution of the normalized spectral density across the current, and (d) modulation level as a function of the angle between wave and current. In (c) the altimeter observations of the normalized variance of surface waves (proportional to the square of the significant wave height) between 27 and 29°N are superimposed for comparison.

$$U(y) = U_0 \exp\left[-\left(\frac{y}{y_b}\right)^2\right], \tag{5}$$

where U_0 is the peak current velocity at the axis, and y_b is a scale width of the current. An example of the current profile $U(y)$, the current shear $U_y(y)$, and the resulting modulation of the wave spectral density, $F(y)/F_0$, is shown in Figs. 2(a)–(c). For these examples, U_0 = 1 and 2 m/s, y_b = 50 km, the initial (unperturbed) wavenumber is k_0 = 0.1 rad/m, and the wave is propagating toward –140° relative to the current axis (0° is toward downstream). Additional calculations for different values of U_0, k_0, and wave propagation angles produce similar modulation results. Figure 2(d) shows the computed modulation level as a function of the angle between wave and current for three combinations of peak current speeds and initial wavenumbers. In Fig. 2(c), field data from Q1 and Q4 are superimposed on the computed curves.

3.2 Discussions

Several observations can be made based on the numerical results shown in Fig. 2. (a) The directional response of the wave modulation by surface current is sinusoidal, with minimal modulation in the cross-current orientation. Waves propagating at a shallow angle in the current direction (near 0°) can be refracted back and are unable to cross the current (e.g., Wang *et al.*, 1994). (b) The amplitude response is linearly proportional to the peak current velocity. And (c) the modulation level increases with wavenumber for a given current strain. All these properties are in accordance with the relaxation theory of wave-current interaction (e.g., Hughes, 1978; Hwang and Shemdin, 1990). The maximum modulation level due to hydrodynamic straining for the winter conditions, with the wave vector at –120° to –180° relative to the Kuroshio axis, is about 10 to 20 percent, assuming that the peak velocity of the Kuroshio is between 1 and 2 m/s. This modulation magnitude is about one third of the observed Kuroshio enhancement of the wave variance (Fig. 2(c)).

Additional mechanisms contributing to the wave-height enhancement, besides wave-current interaction, include the unstable stratification and the spatial distribution of the wind speeds. The effect of wind-speed distribution can be estimated by the growth function of wind-generated surface waves, represented here as a power-law dependence of the dimensionless wave energy on the dimensionless wave frequency (inverse wave age),

$$e_* = R\omega_*^r, \tag{6}$$

where $e_* = \sigma^2 g^2 / U_{10}^4$, $\omega_* = \omega_p U_{10}/g$, $\sigma\,(=H_s/4)$ is the root mean square (RMS) surface displacement, ω_p is the angular frequency of the wave component at the spectral peak and g is the gravitational acceleration. Expressed in dimensional form, the dependence of wave height on wind speed can be written as

$$H_s^2 = 16 R g^{-r-2} U_{10}^{4+r} \omega_p^r. \tag{7}$$

For the purpose of the present discussion, assume that the change in ω_p is relatively small, then the modification of H_s by the change of wind speed can be estimated by $H_s^2 \sim U_{10}^{4+r}$. The exponent r varies from –3.00 to –3.42 based on analyses of fetch-limited wave growth data (e.g., Toba, 1978; Young, 1999; Hwang and Wang, 2004), therefore, $H_s^2 \sim U_{10}^{0.6}$ to $U_{10}^{1.0}$. Using the results between 29° and 28°N shown in Fig. 1(c) to estimate the Kuroshio effects, the wind-speed enhancement by the Kuroshio is about 9 percent in Q1 (U_{10} = 7.8 m/s at 29°N and 8.5 m/s at 28°N), and contributes directly about 5 to 9 percent to the wave-variance enhancement; the observed wave-variance enhancement is about 30 percent (H_s = 1.71 m at 29°N and 1.95 m at 28°N). For Q4, the wind-speed enhancement is about 15 percent (U_{10} = 6.5 m/s at 29°N and 7.5 m/s at 28°N) and makes about a 10 to 15 percent direct contribution; the observed wave-variance enhancement is about 33 percent (H_s = 1.56 m at 29°N and 1.80 m at 28°N). In other words, the direct contribution of the increased wind speed accounts for about 20 to 40 percent of the observed total wave-variance enhancement. As mentioned earlier, the wave-current interaction of contributes a similar level (about one third) (Fig. 2(c)).

The computations performed so far did not consider the effects of thermal stratification, which may provide a similar degree of wave-variance enhancement attributable to the Kuroshio. The growth rate of wind-generated waves under unstable stratification has been observed to be more than twice the growth rate in neutral conditions (Kahma and Calkoen, 1992; Young, 1999). The estimation of the stability effect requires the information of air and water temperatures, and will not be attempted here. However, judging from the calculations shown above, the stability effect on wind-wave generation may contribute about one third to the observed wave-variance enhancement attributable to the Kuroshio influence.

4. Conclusions

The Kuroshio is the major ocean current conveying heat and mass in the Pacific Ocean. It plays a role similar to the Gulf Stream in the Atlantic Ocean. In the East China Sea, the Kuroshio trajectory is relatively stationary, the monsoon patterns dominate, and the boundaries are well defined, making the region an ideal natural laboratory for large scale air-sea-current interaction research. The impact of the Kuroshio on winds and waves has been studied using spaceborne altimeter data. The results show that the Kuroshio exerts a significant influence on winds and waves over a swath about 800-km wide along its path, and increases the average U_{10} by about 20 to 50 percent. The Kuroshio modulations of winds and waves are most prominent in the first and fourth quarters when air-sea temperature contrast is high. In the second and third quarters, when the Kuroshio influence weakens, effects from regional frontal structures become more detectable. The local peaks in the wind-speed modulation match the Yangtze Bank Ring Front and the Shandong Peninsula Front inferred from long-term SST probability studies of the frontal structure in the region (Hickox *et al.*, 2000; Belkin and Cornillon, 2003).

The wave-height distributions display similar patterns to those of the wind-speed distributions. The magnitude of the wave-height enhancement is larger than that attributable to the wind-speed enhancement. In addition to the unstable thermal stratification, it is suggested that the wave-current interaction is another important mechanism boosting the wave-height enhancement. Numerical computations using the action density conservation equation show that the contribution due to wave-current interaction is on the same level as the direct effect of the wind-speed enhancement.

Acknowledgements

This work is supported by the Office of Naval Research (NRL PE61153N). Gregg Jacobs and Bill Teague extracted the wind and wave data from the TOPEX/Poseidon GDR. Pierre Queffeulou and an anonymous reviewer provided valuable comments and suggestions on an earlier version of the manuscript. Their contributions are acknowledged. This is NRL Contribution JA/7330-04-0020.

References

Beardsley, R. C., R. Limeburner, H. Yu and G. A. Cannon (1985): Discharge of the Changjiang (Yangtze River) into the East China Sea. *Cont. Shelf Res.*, **4**, 57–76.

Belkin, I. and P. Cornillon (2003): SST fronts of the Pacific coastal and marginal seas. *Pacific Oceanogr.*, **1**, 90–113.

Freilich, M. H. and P. G. Challenor (1994): A new approach for determining fully empirical altimeter wind speed model functions. *J. Geophys. Res.*, **99**, 25051–25062.

Gower, J. F. R. (1996): Intercomparison of wave and wind data from TOPEX/POSEIDON. *J. Geophys. Res.*, **101**, 3817–3829.

Hickox, R., I. Belkin, P. Cornillon and Z. Shan (2000): Climatology and seasonal variability of ocean fronts in the East China, Yellow and Bohai Seas from satellite SST data. *Geophys. Res. Lett.*, **27**, 2945–2948.

Hughes, B. A. (1978): The effect of internal waves on surface wind waves, 2. Theoretical analysis. *J. Geophys. Res.*, **83**, 455–465.

Hwang, P. A. (1999): Microstructure of ocean surface roughness: A study of spatial measurement and laboratory investigation of modulation analysis. *J. Atmos. Ocean. Tech.*, **16**, 1619–1629.

Hwang, P. A. and O. H. Shemdin (1990): Modulation of short waves by surface currents—a numerical solution. *J. Geophys. Res.*, **95**, 16311–16318.

Hwang, P. A. and W. J. Teague (1998): Technical evaluation of constructing wind and wave climatologies using spaceborne altimeter output, with a demonstration study in the Yellow and East China Seas. Naval Research Laboratory Memo. Rep. NRL/MR/7332-98-8216, 41 pp.

Hwang, P. A. and D. W. Wang (2004): Field measurements of duration-limited growth of wind-generated ocean surface waves at young stage of development. *J. Phys. Oceanogr.*, **34**, 2316–2326; Corrigendum, **35**, 268–270, 2005.

Hwang, P. A., W. J. Teague, G. A. Jacobs and D. W. Wang (1998a): A statistical comparison of wind speed, wave height and wave period derived from satellite altimeters and ocean buoys in the Gulf of Mexico region. *J. Geophys. Res.*, **103**, 10451–10468.

Hwang, P. A., W. J. Teague and G. A. Jacobs (1998b): Spaceborne measurements of Kuroshio modulation of wind and wave properties in the Yellow and East China Seas. *J. Adv. Mar. Sc. and Tech. Soc.*, **4**, 155–164.

Hwang, P. A., S. M. Bratos, W. J. Teague, D. W. Wang, G. A. Jacobs and D. T. Resio (1999): Winds and waves in the Yellow and East China Seas: Spaceborne altimeter measurements and model results. *J. Oceanogr.*, **55**, 307–325.

Kahma, K. K. and C. J. Calkoen (1992): Reconciling discrepancies in the observed growth of wind-generated waves. *J. Phys. Oceanogr.*, **22**, 1389–1405.

Keller, W. C. and J. W. Wright (1975): Microwave scattering and the straining of wind-generated waves. *Radio Sci.*, **10**, 135–147.

Lie, H.-J., C.-H. Cho, J.-H. Lee, P. Niiler and J.-H. Hu (1998): Separation of the Kuroshio water and its penetration onto the continental shelf west of Kyushu. *J. Geophys. Res.*, **103**, 2963–2976.

Lie, H.-J., C.-H. Cho, J.-H. Lee, S. Lee, Y. Tang and E. Zou (2001): Does the Yellow Sea Warm Current really exist as a persistent mean flow? *J. Geophys. Res.*, **106**, 22199–22210.

Longuet-Higgins, M. S. and R. W. Stewart (1960): Changes in the form of short gravity waves on long waves and tidal currents. *J. Fluid. Mech.*, **8**, 565–583.

Nitani, H. (1972): Beginning of the Kuroshio. p. 353–369. In *Kuroshio*, ed. by H. Stommel and K. Yoshida, Univ. Tokyo Press, Tokyo, Japan.

Nonaka, M. and S.-P. Xie (2003) Covariations of sea surface temperature and wind over the Kuroshio and its extension: Evidence for ocean-to-atmosphere feedback. *J. Climate*, **16**, 1404–1413.

Plant, W. J. (1980): On the steady-state energy balance of short gravity wave systems. *J. Phys. Oceanogr.*, **10**, 1340–1352.

Qiu, B. and N. Imasato (1990): A numerical study on the formation of the Kuroshio Counter Current and the Kuroshio Branch Current in the East China Sea. *Cont. Shelf Res.*, **10**, 165–184.

Queffeulou, P. (2003): Long-term quality status of wave height and wind speed measurements from satellite altimeters. *CD-ROM Proc. of the ISOPE Conf.*, Honolulu, Hawaii, U.S.A., May 25–30.

Queffeulou, P. (2004): Long term validation of wave height measurements from altimeters. *Mar. Geodesy.*, **27**, 495–510.

Sun, X.-P. and Y.-F. Su (1994): On the variation of Kuroshio in East China Sea. p. 49–58. In *Oceanology of China Seas*, ed. by D. Zhou, Y.-B. Liang and C. K. Zeng, Kluwer Academic Press, the Netherlands.

Teague, W. J., G. A. Jacobs, D. S. Ko, T. Y. Tang, K.-I. Chang and M.-S. Suk (2003): Connectivity of the Taiwan, Cheju, and Korea Straits. *Cont. Shelf Res.*, **23**, 63–77.

Thompson, D. R. and R. F. Gasparovic (1986): Intensity modulation in SAR images of internal waves. *Nature*, **320**, 345–348.

Toba, Y. (1978): Stochastic form of the growth of wind waves in a single-parameter representation with physical implications. *J. Phys. Oceanogr.*, **8**, 494–507.

Wang, D. W., A. K. Liu, C. Y. Peng and E. A. Meindl (1994): Wave-current interaction near the Gulf Stream during the Surface Wave Dynamics Experiment. *J. Geophys. Res.*, **99**, 5065–5079.

Wang, Y. and D. G. Aubrey (1987): The characteristics of China Coastline. *Cont. Shelf Res.*, **7**, 329–349.

Weissman, D. E. and H. C. Graber (1999): Satellite scatterometer studies of ocean surface stress and drag coefficients using a direct model. *J. Geophys. Res.*, **104**, 11329–11335.

Xie, S.-P., J. Hafner, Y. Tanimoto, W. T. Liu, H. Tokinaga and H. Xu (2002): Bathymetric effect on the winter sea surface temperature and climate of the Yellow and East China Seas. *Geophys. Res. Lett.*, **29**, 2228, doi:10.1029/2002GL015884.

Young, I. R. (1999): *Wind Generated Ocean Waves*. Elsevier, Amsterdam, the Netherlands, 288 pp.